Livestock Science 248 (2021) 104503

Contents lists available at ScienceDirect

Livestock Science

journal homepage: www.elsevier.com/locate/livsci

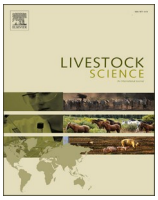

Transcriptome changes in newborn goats' skeletal muscle as a result of maternal feed restriction at different stages of gestation

Thaís C. Costa [a,b], Tiago A.O. Mendes [c], Marta M.S. Fontes [a,b], Mariana M. Lopes [a,b], Min Du [d], Nick V.L. Serão [e], Leticia M.P. Sanglard [e], Francesca Bertolini [d,e,f], Max F. Rothschild [e], Fabyano F. Silva [a], Mateus P. Gionbelli [g], M.S. Duarte [a,b,*]

[a] Department of Animal Science, Universidade Federal de Viçosa, Viçosa, 36570-000, Brazil
[b] Muscle Biology and Nutrigenomics Laboratory, Universidade Federal de Viçosa, Viçosa, 36570-000, Brazil
[c] Department of Biochemistry and Molecular Biology, Universidade Federal de Viçosa, 36570-000, Brazil
[d] Department of Animal Sciences, Washington State University, Pullman, 99164, USA.
[e] Department of Animal Science, Iowa State University, Ames, 50011, USA.
[f] National Institute of Aquatic Resources, Technical University of Denmark, Lyngby, 2800, Denmark
[g] Department of Animal Science, Universidade Federal de Lavras, Lavras, 37200-900, Brazil

HIGHLIGHTS

- Maternal feed restriction during distinct stages of gestation.
- Alterations in offspring's skeletal muscle transcriptome.
- Genes related to satellite cells, insulin sensitivity and composition of intramuscular fat were identified.

ARTICLE INFO

Keywords:
Caprine
Fetal programming
RNA-seq
Muscle metabolism
Undernutrition

ABSTRACT

We investigated how feed restriction at 50% of maintenance requirements during different stages of gestation affects the transcriptome of newborn goats' skeletal muscle. Fourteen pregnant dams were randomly assigned into one of the following dietary treatments: animals fed at 50% of maintenance requirement from 8–84 d of gestation and then fed at 100% of maintenance requirement from day 85 of gestation to parturition (RM, $n = 6$), and animals fed at 100% of maintenance requirement from 8–84 d of gestation and then fed at 50% of maintenance requirement from day 85 of gestation to parturition (MR, $n = 8$). At birth, samples of offspring's *Longissimus* muscle were collected for total RNA extraction and sequencing. Our data showed 66 differentially expressed (DE) genes (FDR < 0.05). A total of 6 genes were upregulated and 60 downregulated (FDR < 0.05) in the skeletal muscle of the newborns resulting from treatment RM compared with MR. Our results suggest that the DE genes upregulated in newborn goats' skeletal muscle from the RM group compared to MR, included genes related to satellite cells, and genes that indicates impaired insulin sensitivity and changes in the composition of intramuscular fat. The DE genes upregulated in newborn goats' skeletal muscle from the MR group compared to RM, are also related to impaired insulin sensitivity, as well as a predominantly oxidative metabolism and cellular oxidative stress. However, protective mechanisms against insulin sensitivity and oxidative stress may have been augmented in the skeletal muscle of offspring from MR treatment compared to RM, in order to maintain cellular homeostasis.

1. Introduction

Fetal programming is based on the hypothesis that environmental stimuli or insults during critical periods of prenatal development may result in permanent changes in the structure and metabolism of an organism, leading to long term consequences (Barker, 1992). Previous

* Corresponding author.
E-mail address: marcio.duarte@ufv.br (M.S. Duarte).

https://doi.org/10.1016/j.livsci.2021.104503
Received 16 October 2020; Received in revised form 26 March 2021; Accepted 29 March 2021
Available online 3 April 2021

studies have shown that the skeletal muscle tissue is affected by maternal feed restriction during gestation (He et al., 2013; Zhang et al., 2015; Paradis et al., 2017). Also, skeletal muscle is one of the most dynamic and plastic tissues (Frontera and Ochala, 2015), extremely susceptible to variations in nutrient supplies during the prenatal stage compared to other vital tissues. The early to mid-gestation is crucial for fetal skeletal muscle development, due to the increase of muscle cells number (hyperplasia), which develops exclusively during the prenatal stage. Concomitantly with secondary myogenesis, adipogenesis begins during mid to late gestation, and although there is evidence of an increase in fat cells after birth, the density of pluripotent cells decreases over time (Du et al., 2010).

Energy metabolism in the offspring's skeletal muscle may also be impaired by maternal nutrition during gestation (Yang et al., 2016), leading to changes in metabolic flexibility, altering the substrate sources for ATP synthesis. These skeletal muscle adaptations are consistent with the hypothesis of the "thrifty phenotype", which postulates that when fetal nutrition is poor, an adaptive response occurs that leads to altered metabolism (Hales and Barker, 2001). For example, Selak et al. (2003) observed a mitochondrial deficiency, which contributes to the decrease of ATP synthesis and compromises glucose transport and utilization in the skeletal muscle of intrauterine growth-retarded rats.

Besides the numerous studies demonstrating alteration in several signaling pathways in the offspring's skeletal muscle, changes in maternal nutrition occurring at different gestational stages can lead to different physiological outcomes in the offspring (Moisá et al., 2015). In this context, real-time qPCR tools are frequently used to determine the relative expression of specific target genes. However, this targeted approach, does not allow for the identification of a global set of genes. Thus, sequencing-based methods, such as RNA-sequencing (RNA-seq) are powerful tools which allow us to evaluate a set of transcripts (transcriptome) in a given tissue, identify new genes and quantify the differentially expressed (DE) genes during development and under different conditions (Wang et al., 2009). Therefore, RNA-seq can be an advantageous tool that can provide more comprehensive knowledge and identify potentially new mechanisms altered by maternal feed restriction observed in the offspring's skeletal muscle.

Our previous study did not identify phenotypic differences in the offspring resulting from maternal feed restriction between the experimental groups (Costa et al., 2019), however, molecular mechanisms may have sustained compensatory growth and contributed to the lack of physical differences. In this context we hypothesized that maternal feed restriction during different stages of gestation alters the transcriptome profile in the skeletal muscle of newborn goats. Thus, the objective of this study was to utilize RNA-seq to identify the global differential gene expression profiles and biological processes of the skeletal muscle in newborn goats affected by maternal feed restriction during the first and second half of gestation.

2. Material and methods

2.1. Animals and sampling

All experimental procedures were approved by the Ethical Committee on Animal Use of the Department of Animal Science at Universidade Federal de Viçosa, Minas Gerais, Brazil (protocol number 09/2017).

The experiment was a continuation of a study investigating the effects of maternal feed restriction during different stages of gestation on the skeletal muscle of the offspring previously described in Costa et al. (2019). Briefly, 14 nulliparous dairy goats, weighing 50 ± 13 kg, at 19 ± 7 months of age (mean ± SD) were submitted to estrus synchronization and artificially inseminated using semen from a single male. The day of insemination was considered day 0 of gestation. The dams were housed in individual pens and submitted to an adaptation period of 7 d receiving the experimental diet and water *ad libitum*. After the adaptation period, the dams were randomly assigned into one of the following dietary treatments: animals fed at 50% of maintenance requirement from 8 to 84 d of gestation and then fed at 100% of maintenance requirement from day 85 of gestation to parturition (term ~ 150d; RM, $n = 6$), and animals fed at 100% of maintenance requirement from 8 to 84 d of gestation and then fed at 50% of maintenance requirement from day 85 of gestation to parturition (MR, $n = 8$). Experimental diets were adjusted weekly based on the body weight and gestational age of the dams and consisted in 111.6 g/kg of crude protein (CP) and 676 g/kg of total digestible nutrients (TDN) on dry matter (DM) basis, composed of corn silage (723 g/kg DM basis), soybean meal (96 g/kg DM basis), ground corn (165 g/kg DM basis) and mineral mixture (16 g/kg DM basis), considering the nutritional requirements for pregnant dairy goats (NRC, 2007).

After birth, male newborn goats were immediately separated from the dams and following approved guidelines stunned using a non-penetrating captive bolt pistol, and exsanguinated. In the case of twins, we selected the heaviest newborn goat. Skeletal muscle samples were collected from the *Longissimus dorsi* muscle and stored in liquid nitrogen for further RNA extraction and sequencing.

2.2. RNA extraction, library generation and sequencing

Total RNA was extracted using RNeasy Fibrous Tissue Mini Kit (Qiagen Inc., Germantown, MD, USA) following the manufacturer's recommendation. The RNA quantification and integrity were determined by Agilent 2100 Bioanalyzer (Agilent Technologies, Inc., Santa Clara, CA, USA). Samples with RNA integrity number (RIN) higher than 8 were sent to Novogene (Sacramento, CA, USA) for library preparation and sequencing on an Illumina HiSeq4000 instrument, following the 150 bp paired-end protocol. An average of approximately 23 million raw reads/sample (150 bp paired-end reads) were generated (Table 1).

2.3. Quality control and assembly

The quality control of raw sequences was evaluated by the FastQC program (Andrews, 2010) and poor sequences were filtered with the Trimmomatic software version 0.36 (Bolger et al., 2014). The illumina adapters were removed, allowing 2 seed mismatches, a palindrome clip threshold of 30, and a simple clip threshold of 10. To remove low quality reads, we used a sliding window trimming that scanned 4 bases each and removed them when the Phred score average was bellow 15. Short reads were also removed. Reads 50 bases or longer were retained after trimming. After the quality control measures, an average of 21 million trimmed reads/sample remained, corresponding to 93% of raw reads (Table 1).

Trimmed reads were aligned to the goat reference genome (*Capra hircus*, assembly ARS1) available at NCBI (www.ncbi.nlm.nih.gov) with ID GCA_001704415.1 using TopHat 2.1.1 software (Trapnell et al., 2009) with Bowtie2 (Langmead and Salzberg, 2012) for alignment. An average of 76% of trimmed reads were successfully mapped (Table 1).

2.4. Differential expression analysis

The Cuffdiff tool (Cufflinks 2.2.1) was used to count reads, normalize transcript expression by fragments per kilobase of transcript model per million reads mapped (FPKM), and identify the differentially expressed genes between treatments. Input included the mapped reads, the indexed genome (generated by the Bowtie2 software) and the reference annotation file. Cuffdiff uses a model for fragment counts based on the beta negative binomial distribution to control cross-replicate variability and read mapping ambiguity. The *P*-values reported by Cufffdiff were corrected for multiple testing by using the false discovery rate (FDR) method (Benjamini and Hochberg, 1995), and differentially expressed (DE) genes were deemed significant when FDR < 0.05. The data quality assessment of principal component analysis (PCA) from the RNAseq

Table 1
Summary of sequenced reads, trimmed reads and mapped reads to the goat reference genome.

Treatment	Sample	Total Reads	Trimmed Reads	% Trimmed Reads	Mapped Reads	% Mapped Reads
MR	1	22,656,017	21,344,634	94.2	F: 17,401,220	81.5
					R: 16,797,503	78.7
	2	23,128,719	20,057,993	86.7	F: 15,560,823	77.6
					R: 15,051,444	75.0
	3	21,494,772	20,199,413	94.0	F: 15,395,237	76.2
					R: 14,913,742	73.8
	4	28,790,577	27,141,345	94.3	F: 20,624,787	76.0
					R: 19,967,572	73.6
	5	21,449,097	20,295,123	94.6	F: 17,479,414	86.1
					R: 16,903,700	83.3
	6	18,219,469	17,046,120	93.6	F: 12,508,113	73.4
					R: 4842,492	28.4
	7	25,875,331	24,188,442	93.5	F: 19,890,066	82.2
					R: 19,251,243	79.6
	8	27,355,478	25,047,818	91.6	F: 18,877,288	75.4
					R: 18,189,586	72.6
RM	1	20,195,795	19,068,867	94.4	F: 15,238,057	79.9
					R: 14,766,121	77.4
	2	23,001,254	21,695,246	94.3	F: 17,309,988	79.8
					R: 16,718,451	77.1
	3	21,389,732	20,072,421	93.8	F: 16,067,259	80.0
					R: 15,505,893	77.2
	4	21,483,827	20,191,419	94.0	F: 16,017,808	79.3
					R: 15,489,336	76.7
	5	25,402,784	23,967,043	94.3	F: 19,699,811	82.2
					R: 19,017,998	79.4
	6	25,070,539	23,443,609	93.5	F: 18,109,868	77.2
					R: 17,540,294	74.8

MR = treatment maintenance-restriction; RM = treatment restriction-maintenance; *F* = forward; *R* = reverse.

analysis was performed using R package (v 3.4.4) (Team, 2013) and plotted using the GraphPad Prism software (version 5.01 for Windows, GraphPad Software, San Diego California USA, www.graphpad.com).

2.5. Gene ontology (GO) and network analyses

Gene Ontology (GO) enrichment and network analyses were built using the ClueGo 2.5.3 (Bindea et al., 2009) application from Cytoscape 3.7.2 (https://cytoscape.org). We assessed the enriched biological processes shared by the DE genes identified in both treatments based on an unilateral hypergeometric test and Benjamini-Hochberg correction (Bei and Hong, 2013; Lewin and Grieve, 2006). Only the biological processes and molecular functions identified with a FDR < 0.05 were considered. The edges connecting the nodes were based on the Kappa statistic (Kappa score = 0.4) (Huang et al., 2009; McHugh, 2012).

3. Results

3.1. Differential gene expression in newborn goats' skeletal muscle

From a total of 20,359 transcripts obtained in the skeletal muscle of newborn goats, 3.8% (766) and 5.6% (1146) of the transcripts were found exclusively in the treatments RM and MR, respectively. These exclusive genes were not explored in the present study, due to the fact that the GO, pathways, and network analyses showed that the same pathway (KEGG pathway) was enriched in both treatments, while no GO was associated to the exclusive genes. Despite the difference in the pools of exclusive genes between the treatments RM and MR, the pathway analysis indicated that neuroactive ligand-receptor pathways (oas04080) is enriched in both treatment groups (RM FDR = 0.0013; MR FDR = 2.35E-06). For differential expression analyses, we tested a total of 18,447 transcripts (90.6% from the total) corresponding to the common transcripts present in both treatments. By using a FDR adjusted cutoff of 0.05, a total of 66 genes showed differential expression between the treatments (Table 2). Particularly, six genes were upregulated and 60 downregulated in RM compared with MR (Table 2; Fig. 1).

3.2. Gene set enrichment analyses

We performed enrichment analyses of the DE genes, in order to assess the biological processes (BP), and molecular functions (MF) that could be differentially regulated between treatments. Upregulated genes (FDR < 0.05) did not share common BP or MF, and therefore, individual gene function will be further discussed. The six upregulated (FDR < 0.05) genes in RM in relation to MR, were: *CYTL1* (cytokine like 1), *LOC102180330* (myelin P2 protein), *LOC108637521* (uncharacterized), and *LOC108637838* (glutathione S-transferase theta-1), *NPNT* (nephronectin), and *UGT8* (UDP glycosyltransferase 8).

From the 60 downregulated genes (FDR < 0.05) in RM in relation to MR, 21 genes were assigned to BP, sub BP, and MF, according to the previous established criteria in ClueGO (FDR< 0.05; Kappa score = 0.4). Significant BP (FDR < 0.05; Table 3) are related to skeletal muscle tissue development (*ATF3, BTG2, FOS, MAFF*, and *METTL21C*), muscle cell proliferation (*CNN1, HMOX1, NR4A3, PPARD*, and *TRIB1*), gluconeogenesis (*ATF3, LOC102191654, PCK2*, and *SESN2*), cellular response to metal ion (*FOS, HMOX1, JUNB*, and *LOC102184306*), regulation of extrinsic apoptotic signaling pathway via death domain receptor (*ATF3, HMOX1*, and *ITPRIP*) and positive regulation of myeloid leukocyte differentiation (*FOS, TRIB1*, and *RUNX1*; Fig. 2). The enriched sub BP (FDR < 0.05; Table 3) are related to fatty acid oxidation (*NR4A3, PPARD*, and *SESN2*), glucose transmembrane transport (*NR4A3, SESN2*, and *TRIB3*), regulation of smooth muscle cell proliferation (*CNN1, HMOX1, NR4A3*, and *TRIB1*), regulation of extrinsic apoptotic signaling pathway (*ATF3, HMOX1, HYAL2, ITPRIP*, and *TNFRSF12A*) and positive regulation of extrinsic apoptotic signaling pathway (*ATF3, HYAL2*, and *TNFRSF12A*; Fig. 2). The enriched MF (FDR < 0.05; Table 3) are related to nuclear receptor activity (*NR4A2, NR4A3*, and *PPARD*), and protein kinase inhibitor activity (*HYAL2, ITPRIP*, and *TRIB1;* Fig. 2). The downregulated genes, represented as triangles, bonded with their respective enriched biological process and molecular function, represented as circles, can be better visualized in Fig. 2.

Table 2
Differentially expressed genes in the skeletal muscle of the offspring.

Gene symbol	NCBI ID	Gene description	MR (FPKM)	RM (FPKM)	log2(fold change)[1]	FDR[2]
CYTL1	102,190,869	cytokine like 1	1.06	4.78	2.18	1.36E-02
LOC102180330	102,180,330	myelin P2 protein	2.21	7.51	1.77	1.36E-02
UGT8	102,174,638	UDP glycosyltransferase 8	0.69	1.96	1.51	1.36E-02
NPNT	102,172,699	nephronectin	1.49	3.86	1.38	1.36E-02
LOC108637521	108,637,521	uncharacterized	2.54	5.68	1.16	1.36E-02
LOC108637838	108,637,838	glutathione S-transferase theta-1	28.37	59.34	1.06	1.36E-02
RAB11FIP5	102,186,696	RAB11 family interacting protein 5	12.38	6.35	−0.96	4.62E-02
JUNB	102,181,201	JunB proto-oncogene, AP-1 transcription factor subunit	30.97	15.74	−0.98	3.15E-02
SLC35E4	102,170,260	solute carrier family 35 member E4	86.10	43.72	−0.98	2.22E-02
KLF15	102,179,715	Kruppel like factor 15	100.24	50.77	−0.98	3.93E-02
TRIB1	102,172,644	tribbles pseudokinase 1	20.20	10.21	−0.98	2.22E-02
SOX18	106,502,775	SRY-box transcription factor 18	43.41	21.50	−1.01	2.22E-02
HYAL2	102,172,212	hyaluronidase 2	27.15	13.20	−1.04	3.93E-02
ID1	102,182,889	inhibitor of DNA binding 1, HLH protein	46.45	22.37	−1.05	1.36E-02
MAFF	102,182,388	MAF bZIP transcription factor F	67.94	32.57	−1.06	2.22E-02
CREM	100,861,259	cAMP responsive element modulator	67.23	32.03	−1.07	1.36E-02
ADRB2	102,179,381	adrenoceptor beta 2	10.28	4.88	−1.08	3.15E-02
ZSWIM4	102,174,646	zinc finger SWIM-type containing 4	3.51	1.60	−1.14	2.22E-02
SGK1	102,176,607	serum/glucocorticoid regulated kinase 1	8.53	3.84	−1.15	2.22E-02
METRNL	102,173,882	meteorin like, glial cell differentiation regulator	26.59	11.96	−1.15	1.36E-02
PPARD	102,174,518	peroxisome proliferator activated receptor delta	26.81	11.86	−1.18	1.36E-02
LOC108634753	108,634,753	collagen alpha-1(I) chain	49.65	21.18	−1.23	1.36E-02
SIK1	102,191,654	salt inducible kinase 1	48.79	20.41	−1.26	1.36E-02
CNN1	102,190,599	calponin 1	12.88	5.37	−1.26	1.36E-02
LOC102188626	102,188,626	cytospin-B	11.62	4.79	−1.28	1.36E-02
LOC102184306	102,184,306	ras GTPase-activating protein 4	3.77	1.54	−1.29	2.22E-02
BTG2	102,187,789	BTG anti-proliferation factor 2	32.44	13.27	−1.29	1.36E-02
ATF3	102,183,991	activating transcription factor 3	100.35	40.49	−1.31	4.62E-02
SNAI3	102,188,886	snail family transcriptional repressor 3	3.44	1.27	−1.44	2.22E-02
ITPRIP	102,190,930	inositol 1,4,5-trisphosphate receptor interacting protein	13.30	4.84	−1.46	1.36E-02
RFLNB	102,173,226	refilin B	5.95	2.15	−1.47	1.36E-02
C15H11orf96	102,181,701	chromosome 15 C11orf96 homolog	63.85	22.02	−1.54	1.36E-02
PCK2	102,179,952	phosphoenolpyruvate carboxykinase 2, mitochondrial	6.34	2.14	−1.57	1.36E-02
FOS	102,171,520	Fos proto-oncogene, AP-1 transcription factor subunit	133.51	44.15	−1.60	1.36E-02
HIP1R	102,178,295	huntingtin interacting protein 1 related	9.33	3.05	−1.61	3.93E-02
CREB5	102,190,378	cAMP responsive element binding protein 5	4.32	1.39	−1.64	4.62E-02
CSRNP1	102,186,348	cysteine and serine rich nuclear protein 1	32.27	10.05	−1.68	1.36E-02
AMPD3	102,176,807	adenosine monophosphate deaminase 3	21.78	6.74	−1.69	1.36E-02
HMOX1	100,860,951	heme oxygenase 1	65.29	19.88	−1.72	1.36E-02
HSPA6	102,185,412	heat shock protein family A (Hsp70) member 6	2.46	0.73	−1.76	2.22E-02
PSPH	102,184,397	phosphoserine phosphatase	10.42	3.07	−1.77	1.36E-02
RRAD	102,175,153	RRAD, Ras related glycolysis inhibitor and calcium channel regulator	301.21	85.57	−1.82	1.36E-02
NR4A3	102,188,043	nuclear receptor subfamily 4 group A member 3	3.64	1.02	−1.84	1.36E-02
TNFRSF12A	102,177,022	TNF receptor superfamily member 12A	234.70	65.34	−1.84	1.36E-02
LOC102168687	102,168,687	interferon-induced protein with tetratricopeptide repeats 1	0.93	0.22	−2.07	2.22E-02
METTL21C	102,180,054	methyltransferase like 21C	5.87	1.35	−2.12	1.36E-02
RUNX1	102,178,020	RUNX family transcription factor 1	2.52	0.58	−2.13	4.62E-02
ADAMTS4	102,176,281	ADAM metallopeptidase with thrombospondin type 1 motif 4	2.13	0.48	−2.16	1.36E-02
TMEM154	102,188,161	transmembrane protein 154	1.84	0.41	−2.17	3.93E-02
SLC16A10	102,181,685	solute carrier family 16 member 10	8.20	1.76	−2.22	1.36E-02
TRIM63	102,172,216	tripartite motif containing 63	758.52	162.15	−2.23	1.36E-02
HSD17B7	102,179,058	hydroxysteroid 17-beta dehydrogenase 7	3.00	0.62	−2.28	1.36E-02
ARID5A	102,174,482	AT-rich interaction domain 5A	9.82	1.88	−2.38	1.36E-02
LOC102171344	102,171,344	uncharacterized	4.41	0.84	−2.40	1.36E-02
NTSR2	102,186,972	neurotensin receptor 2	3.85	0.73	−2.41	1.36E-02
NR4A2	102,169,808	nuclear receptor subfamily 4 group A member 2	6.98	1.24	−2.50	1.36E-02
RAB20	102,183,802	RAB20, member RAS oncogene family	41.48	6.74	−2.62	1.36E-02
LOC102175876	102,175,876	hemoglobin subunit beta-A-like	7.70	1.23	−2.64	1.36E-02
TNFRSF6B	102,169,607	TNF receptor superfamily member 6b	6.18	0.96	−2.69	1.36E-02
PTX3	102,179,601	pentraxin 3	10.87	1.58	−2.78	3.15E-02
TRIB3	102,181,514	tribbles pseudokinase 3	3.52	0.44	−3.01	1.36E-02
LOC102188072	102,188,072	metallothionein-2	75.95	7.52	−3.34	1.36E-02
CHAC1	102,173,008	ChaC glutathione specific gamma-glutamylcyclotransferase 1	6.89	0.54	−3.68	1.36E-02
BDNF	102,180,782	brain derived neurotrophic factor	5.55	0.40	−3.81	1.36E-02
SESN2	102,175,632	sestrin 2	5.48	0.30	−4.20	1.36E-02
FOSL1	102,172,040	FOS like 1, AP-1 transcription factor subunit	8.81	0.21	−5.39	1.36E-02

MR = Maintenance-restriction; RM = Restriction-maintenance; FPKM = Fragments per kilobase of transcript model per million reads.
1Positive and negative log2 (fold change) indicates genes up and downregulated in the treatment RM compared to MR.
2FDR: False discovery rate; Adjusted P-value for multiple testing with the Benjamini–Hochberg procedure.

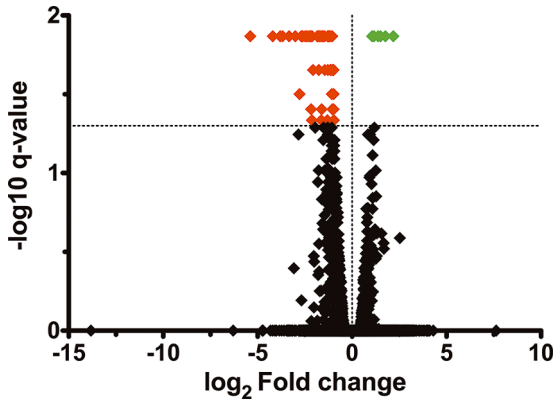

Fig. 1. Volcano plot comparing gene expression fold changes (FC) between treatments (ratio RM /MR). Differentially expressed (DE) genes (FDR < 0.05) are highlighted in red and green. DE genes highlighted in green are upregulated and DE genes highlighted in red are downregulated.

Table 3
Biological processes and Molecular functions associated with the downregulated genes in the skeletal muscle of the offspring from treatment RM compared to the treatment MR.

GO ID	GO Term	FDR[1]	Associated Genes[2]
Biological Process			
GO:0,033,002	muscle cell proliferation	1.54E-04	[CNN1, HMOX1, NR4A3, PPARD, TRIB1]
GO:0,048,660	regulation of smooth muscle cell proliferation	2.08E-04	[CNN1, HMOX1, NR4A3, TRIB1]
GO:0,006,094	gluconeogenesis	2.29E-04	[ATF3, LOC102191654, PCK2, SESN2]
GO:0,007,519	skeletal muscle tissue development	2.29E-04	[ATF3, BTG2, FOS, MAFF, METTL21C]
GO:1,902,041	regulation of extrinsic apoptotic signaling pathway via death domain receptors	3.81E-04	[ATF3, HMOX1, ITPRIP]
GO:2,001,238	positive regulation of extrinsic apoptotic signaling pathway	3.94E-04	[ATF3, HYAL2, TNFRSF12A]
GO:0,071,248	cellular response to metal ion	4.08E-04	[FOS, HMOX1, JUNB, LOC102184306]
GO:2,001,236	regulation of extrinsic apoptotic signaling pathway	4.21E-04	[ATF3, HMOX1, HYAL2, ITPRIP, TNFRSF12A]
GO:0,002,763	positive regulation of myeloid leukocyte differentiation	6.95E-04	[FOS, RUNX1, TRIB1]
GO:0,019,395	fatty acid oxidation	1.33E-03	[NR4A3, PPARD, SESN2]
GO:1,904,659	glucose transmembrane transport	1.33E-03	[NR4A3, SESN2, TRIB3]
Molecular Function			
GO:0,004,860	protein kinase inhibitor activity	3.98E-04	[HYAL2, ITPRIP, TRIB1]
GO:0,004,879	nuclear receptor activity	3.98E-04	[NR4A2, NR4A3, PPARD]

[1] FDR: False discovery rate; Adjusted P-value for multiple testing with the Benjamini–Hochberg procedure.
[2] Downregulated genes in treatment RM compared to MR treatment.

4. Discussion

Maternal plane of nutrition programs fetal growth and development, through epigenetic modulation, leading to changes in gene or protein expression. Changes in the offspring phenotype may vary according to the type and extent of maternal insult during gestation. Studies have suggested that an adequate plane of nutrition during gestation after a period of restriction may sustain a state of compensatory growth and normalize the phenotype between restricted and non-restricted offspring (Costa et al., 2019; Gonzalez et al., 2013). Although there may be no apparent fetal phenotypic responses to maternal feed restriction, the offspring may show adaptation mechanisms at molecular levels (Paradis et al., 2017). In the current study, the RNA-seq technology allowed the identification of DE genes in the skeletal muscle of the offspring from dams which experienced two different feed restriction protocols during gestation. The effect of maternal feed restriction was previously reported by Costa et al. (2019). The dams which experienced feed restriction during the first or second half of gestation presented loss in the average daily gain of maternal tissues in the respective periods of restriction. Since the newborns were harvested soon after birth for sampling, the discussion is based on sequencing data of the newborns' skeletal muscle to predict postnatal phenotype.

Among the DE genes, *CYTL1, NPNT,* and *UGT8* were upregulated in the skeletal muscle of the offspring from treatment RM compared to MR. *CYTL1* is widely expressed in a variety of cells, including CD34+ hematopoietic stem cells (Yang et al., 2018). Beauchamp et al. (2000) showed that CD34 is also present in the majority of quiescent skeletal muscle satellite cells. When required, satellite cells undergo the process of activation, proliferation, differentiation, and fusion (Chargé and Rudnicki, 2004). During the process of differentiation, the abundance of NPNT, an extracellular matrix protein involved in cellular adhesion is increased and it stimulates the myoblast fusion (Sunadome et al., 2011). The upregulation of *CYTL1* in the offspring resulting from mothers that experienced feed restriction during early-to-mid gestation (RM) in comparison to MR may have provided greater number of quiescent satellite cells and the upregulation of *NPNT* may contribute to myoblast fusion and consequently form new myofibers later in life. Moreover, it was also demonstrated that *CYTL1* and *NPNT* may contribute to the level and composition of fatty acid in the skeletal muscle. Low marbled meat presented high expression of *NPNT* (Clark et al., 2011). While the downregulation of *CYTL1* was observed in broilers that displayed high polyunsaturated fatty acids percentage in the skeletal muscle (Yang et al., 2018). Thus, the upregulation of *CYTL1* and *NPNT* may contribute to the decrease in the intramuscular fat deposition accompanied by the decrease in polyunsaturated fatty acid concentration in the skeletal muscle of the offspring from RM compared to MR group.

Evaluating the effects of calorie restriction in rats' skeletal muscle, Obanda et al. (2015) observed that, although there was no reduction of lipid deposition in the skeletal muscle of calorie-restricted rats, sphingolipids metabolism was altered and caused effects in insulin sensitivity. The enzyme *UGT8* catalyzes the transfer of galactose to ceramide to synthesize the sphingolipids galactosylceramide (GalCer) (Marcus and Popko, 2002), which is negatively correlated with insulin sensitivity and positively with pro-inflammatory responses (Pillon et al., 2018). In this context, the upregulation of *UGT8* in the skeletal muscle of RM offspring compared to MR group, could cause insulin resistance, which can be characterized for many factors including impaired glucose transport, glucose phosphorylation, and reduced glucose oxidation and glycogen synthesis (Abdul-Ghani and Defronzo, 2010). The enzyme responsible for glucose phosphorylation in the skeletal muscle is HKII. Although, insulin resistance would lead to decrease HKII activity, our previous study (Costa et al., 2019) showed that *HKII* mRNA abundance was increased in the treatment RM compared to MR. Due to such inconsistency the main role of the gene *UGT8* in the skeletal muscle of feed restricted offspring needs further investigations.

Among the downregulated genes in the skeletal muscle of the offspring from treatment RM compared to MR, methyltransferase like 21C (*METTL21C*) is involved in the biological process of skeletal muscle tissue development. The protein methyltransferases perform multiple functions in the muscle, modifying histones and cytoplasmic proteins (for review see: Clarke, 2013). Elevated abundance of the protein METTL21C regulates protein turnover during various situations, such as,

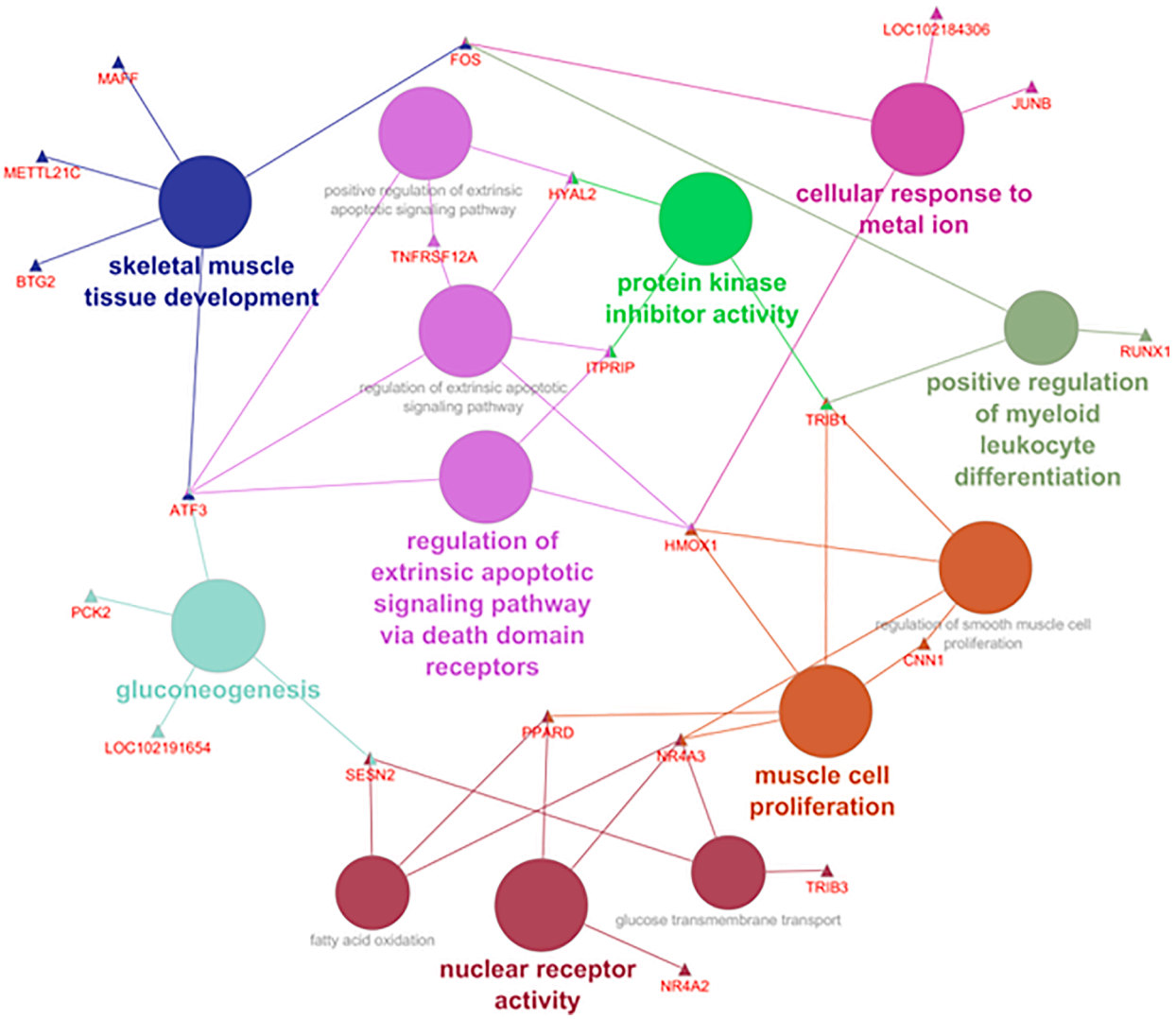

Fig. 2. Analyses of the enriched biological process and molecular function the downregulated genes in treatment RM compared to treatment MR. Network connecting the downregulated genes (triangles) with the enriched biological processes (circles). The node colors represent the functional group and nodes size represents the term enrichment significance. The most significant (FDR < 0.05) term in the group is labeled with colorful and bold letters, while sub biological processes are labeled with black and small letters.

hypertrophy and starvation (Wiederstein et al., 2018). There is evidence that *METTL21C* expression is absent during myogenesis, is limited to mature type I myofibers (Wang et al., 2019a), and also the protein encoded by the gene *METTL21C* correlates positively with the amount of slow type I fibers (Wiederstein et al., 2018), which have oxidative characteristics. The lack of difference between treatments regarding the expression of the marker of slow type I fibers observed in our previous study (Costa et al., 2019) may be due to the molecular markers that was chosen (*MYH1*), since *METTL21C* expression is restricted to slow MYH7-positive muscle fibers (Wiederstein et al., 2018). Regarding muscle fiber types, the nuclear transcription factor peroxisome proliferator-activated delta (*PPARδ*), downregulated in skeletal muscle of the offspring from treatment RM compared to MR participates in biological processes related to muscle cell proliferation and fatty acid oxidation. Specifically, the protein encoded by *PPARδ* regulates the skeletal muscle fiber phenotype, coordinating the increase in oxidative enzymes and mitochondrial biogenesis, and, consequently, an increase in the proportion of slow type I fibers (Wang et al., 2004). Moreover, PPARδ regulates the transcription of the mitochondrial phosphoenolpyruvate carboxykinase 2 (*PCK2*) (Idrees et al., 2019), also downregulated in the skeletal muscle of the offspring from treatment RM compared to MR. *PCK2* is related to the gluconeogenesis biological process and is an important enzyme that catalyzes the conversion of mitochondrial oxaloacetate to phosphoenolpyruvate, which is involved in glucose synthesis (gluconeogenesis) or in generating precursors for triglyceride synthesis (glyceroneogenesis) (Beale et al., 2007). Hence, PCK2 plays an important role in both energy metabolism and lipid homeostasis. Taken together, the skeletal muscle of the offspring resulting from maternal feed restriction during mid-to-late (MR) gestation, may have a greater proportion of oxidative myofibers compared to RM. Moreover, the percentage of number and area of type I fibers was positively correlated with intramuscular fat (IMF) content (Joo et al., 2017), which would possibly contribute for increase in IMF content and consequently the improvement in meat quality in MR offspring compared to RM group.

Among the downregulated genes in RM compared to MR, tribbles homolog 3 (*TRIB3*) and tribbles homolog 1 (*TRIB1*) genes are related with the glucose transmembrane transport and muscle cell proliferation biological processes, respectively. Both increases and decreases in glucose concentration in a skeletal muscle cell line were capable of enhancing the expression of tribbles homolog 3 (TRIB3), considered an energy sensor (Liu et al., 2010). Additionally, TRIB3 overexpression inhibits the downstream insulin signaling pathway, reducing the glucose transport system (Liu et al., 2010). As a consequence of impaired glucose

oxidation, TRIB3, and TRIB1 contribute to the modulating of skeletal muscle differentiation and lipid metabolism (Prudente et al., 2012). Unlike *TRIB3*, other mechanisms that optimize glucose utilization in order to return to energy homeostasis appear to be activated in the skeletal muscle of the offspring in response to maternal feed restriction during mid-to-late gestation (MR). This is the case for the orphan nuclear receptor subfamily 4 group A member 3 (NR4A3) gene, downregulated in RM compared to MR, which is involved in the regulation of genes that control glucose and fatty acid utilization in the skeletal muscle, in a way that improves insulin sensitivity, glucose tolerance and transport and also results in reduced fat deposition (Zhang et al., 2014). Thus, the mechanisms involved by *TRIB3* of reducing glucose transport and oxidation accompanied by the action of *NR4A3* which in contrast improves glucose utilization may characterize an attempt to reach energy balance in the skeletal muscle of the offspring from MR compared to RM group.

The high metabolic capacity of skeletal muscle makes it susceptible to oxidative stress, characterized by an imbalance between reactive metabolites (ROS) and antioxidants, leading to cellular damage and altering production of macromolecules including lipids, DNA, and proteins (Meng and Yu, 2010). Also, increased ROS production impairs the regenerative capacity of satellite cells (Fulle et al., 2004). A number of downregulated genes in RM compared to MR are associated with oxidative stress response and protective mechanisms that ensure cell survival. The expression of B-cell translocation 2 (*BTG2*), and Tumor necrosis factor (TNF) receptor superfamily member 12A (*TNFRSF12A*) appears to be associated with the increase in cellular oxidative stress, while Sestrin2 (*SESN2*), Heme oxygenase-1 (*HMOX1*), and the transcriptional factors *MAFF, FOS* and *JUNB* are known to be activated in response to oxidative stress and their activation results in decreased ROS production and promote cell survival. BTG2 expression is upregulated during oxidative stress (Imran and Lim, 2013; Rouault et al., 1996), has an antiproliferative role, controlling cell-cycle, apoptosis, and differentiation (Yuniati et al., 2019). Apoptosis mediated by BTG2 appears to take place through activation of the nuclear factor kappaB (NFκB) pathway (Imran and Lim, 2013). Upstream of the NFκB pathway, signaling transduction can be initiated by the activation of the transmembrane family receptors TNFRSF12A (Blanco-Colio, 2014). In differentiating muscle cells, NFκB and activating protein −1 (AP-1) transcription factor family, that consists of JUN, FOS, MAF and ATF are activated in response to oxidative stress (Zhou et al., 2001). The induction of SESN2 mediated by oxidative stress, DNA damage, hypoxia, and nutritional stress, triggers homeostatic mechanisms such as the downregulation of ROS accumulation (Wang et al., 2019b). Moreover, the biological effects of HMOX1 are associated with a decrease in ROS production, improvement of cell survival, and proliferation under oxidative stress (Kozakowska et al., 2012). Due to the increased expression of established markers of cellular protective pathways against excessive oxidative stress in the skeletal muscle of MR newborns, we hypothesize that they experience higher levels of oxidative stress, and therefore activate protective mechanisms against it, when compared to the skeletal muscle of newborns resulting from maternal feed restriction during early-to-mid gestation.

5. Conclusion

In summary, the findings of the present study demonstrate that maternal feed restriction during different stages of gestation alters the transcriptome of the newborn goats' skeletal muscle. It is important to highlight that feed restriction, at some point, affected the expression of genes associated with the skeletal muscle development and metabolism. Specifically, feed restriction in the first half in comparison to feed restriction in the second half of gestation may have resulted in reduced myoblast differentiation resulting in greater number of satellite cells in the postnatal period. Also, based on the upregulated genes, maternal feed restriction during the first half of gestation may have impact in insulin sensitivity, compromise intramuscular fat accumulation and fatty acid composition in the skeletal muscle of the offspring, in comparison to feed restriction in the second half of gestation.

Compared to feed restriction during the first half of gestation, the offspring resulting from maternal feed restriction during the second half of gestation also may have impaired insulin sensitivity in the skeletal muscle, however, it appears that protective mechanisms may be activated in order to improve insulin sensitivity and glucose tolerance. Moreover, feed restriction during the second half of gestation may have resulted in increased oxidative metabolism as compared to feed restriction during the first half of gestation, and generated a response against the oxidative stress, promoting cell survival and homeostasis in the skeletal muscle of the offspring.

Credit authorship contribution statement

TCC: Methodology, Software, Validation, Formal analysis, Investigation, Writing - Original Draft, Writing - Review & Editing. **TAOM:** Methodology, Software, Validation, Formal analysis, Resources, Data Curation, Writing - Review & Editing. **MMSF:** Writing - Review & Editing. **MML**: Investigation, Writing - Review & Editing. **MD:** Writing - Review & Editing. **NVLS:** Investigation, Resources, Writing - Review & Editing. **LMPS:** Investigation, Writing - Review & Editing. **FB:** Writing - Review & Editing. **MFR:** Investigation, Resources, Writing - Review & Editing. **FFS:** Investigation, Resources, Writing - Review & Editing. **MPG:** Methodology, Writing - Review & Editing. **MSD:** Conceptualization, Methodology, Investigation, Resources, Supervision, Project administration, Funding acquisition.

Declaration of Competiting Interest

The authors declare that they have no competing interests.

Acknowledgements

This research was supported by funding from CNPq – Conselho Nacional de Desenvolvimento Científico (Grant#311883/2018–4) e Tecnológico, CAPES – Coordenação de Aperfeiçoamento de Pessoal de Nível Superior (Grant#001), FAPEMIG – Fundação de Amparo à Pesquisa de Minas Gerais (Grant#APQ-02496–17) and INCT-CA - Instituto Nacional de Ciência e Tecnologia de Ciência Animal. The funding body had no role in the design of the study and collection, analyses, and interpretation of data and in writing the manuscript.

References

Abdul-Ghani, M.A., Defronzo, R.A., 2010. Pathogenesis of insulin resistance in skeletal muscle. J. Biomed. Biotechnol. https://doi.org/10.1155/2010/476279.

Andrews, S., 2010. FastQC: A quality Control Tool For High Throughput Sequence Data.

Barker, D.J., 1992. The fetal origins of adult hypertension. J. Hypertens. 10 (Suppl. 7), S39–S44.

Beale, E.G., Harvey, B.J., Forest, C., 2007. PCK1 and PCK2 as candidate diabetes and obesity genes. Cell Biochem. Biophys. 48, 89–95. https://doi.org/10.1007/s12013-007-0025-6.

Beauchamp, J.R., Heslop, L., Yu, D.S.W., Tajbakhsh, S., Kelly, R.G., Wernig, A., Buckingham, M.E., Partridge, T.A., Zammit, P.S., 2000. Expression of CD34 and Myf5 defines the majority of quiescent adult skeletal muscle satellite cells. J. Cell Biol. 151, 1221–1233. https://doi.org/10.1083/jcb.151.6.1221.

Bei, Y., Hong, P., 2013. A novel approach to minimize false discovery rate in genome-wide data analysis. BMC Syst. Biol. 7, S1. https://doi.org/10.1186/1752-0509-7-S4-S1.

Benjamini, Y., Hochberg, Y., 1995. Controlling the false discovery rate: a practical and powerful approach to multiple testing. J. R. Stat. Soc. Ser. B 57, 289–300.

Bindea, G., Mlecnik, B., Hackl, H., Charoentong, P., Tosolini, M., Kirilovsky, A., Fridman, W.H., Pagès, F., Trajanoski, Z., Galon, J., 2009. ClueGO: a Cytoscape plug-in to decipher functionally grouped gene ontology and pathway annotation networks. Bioinformatics 25, 1091–1093. https://doi.org/10.1093/bioinformatics/btp101.

Blanco-Colio, L.M., 2014. TWEAK/Fn14 axis: a promising target for the treatment of cardiovascular diseases. Front. Immunol. 5, 1–13. https://doi.org/10.3389/fimmu.2014.00003.

Bolger, A.M., Lohse, M., Usadel, B., 2014. Trimmomatic: a flexible trimmer for Illumina sequence data. Bioinformatics 30, 2114–2120. https://doi.org/10.1093/bioinformatics/btu170.

Chargé, S.B.P., Rudnicki, M.a, 2004. Cellular and molecular regulation of muscle regeneration. Physiol. Rev. 84, 209–238. https://doi.org/10.1152/physrev.00019.2003.

Clark, D.L., Boler, D.D., Kutzler, L.W., Jones, K.A., McKeith, F.K., Killefer, J., Carr, T.R., Dilger, A.C., 2011. Muscle gene expression associated with increased marbling in beef cattle. Anim. Biotechnol. 22, 51–63. https://doi.org/10.1080/10495398.2011.552031.

Clarke, S.G., 2013. Protein methylation at the surface and buried deep: thinking outside the histone box. Trends Biochem. Sci. 38, 243–252. https://doi.org/10.1016/j.tibs.2013.02.004.

Costa, T.C., Moura, F.H., Souza, R.O., Lopes, M.M., Fontes, M.M.S., Serão, N.V.L., Sanglard, L.P., Du, M., Gionbelli, M.P., Duarte, M.S., 2019. Effect of maternal feed restriction in dairy goats at different stages of gestation on skeletal muscle development and energy metabolism of kids at the time of births. Anim. Reprod. Sci. 206, 46–59. https://doi.org/10.1016/j.anireprosci.2019.05.006.

Du, M., Tong, J., Zhao, J., Underwood, K.R., Zhu, M., Ford, S.P., Nathanielsz, P.W., 2010. Fetal programming of skeletal muscle development in ruminant animals. J. Anim. Sci. 88 (Supp. 13), E51–E60. https://doi.org/10.2527/jas.2009-2311.

Frontera, W.R., Ochala, J., 2015. Skeletal Muscle: a Brief Review of Structure and Function. Calcif. Tissue Int. 96, 183–195. https://doi.org/10.1007/s00223-014-9915-y.

Fulle, S., Protasi, F., Di Tano, G., Pietrangelo, T., Beltramin, A., Boncompagni, S., Vecchiet, L., Fanò, G., 2004. The contribution of reactive oxygen species to sarcopenia and muscle ageing. Exp. Gerontol. 39, 17–24. https://doi.org/10.1016/j.exger.2003.09.012.

Gonzalez, J.M., Camacho, L.E., Ebarb, S.M., Swanson, K.C., Vonnahme, K.A., Stelzleni, A. M., Johnson, S.E., 2013. Realimentation of nutrient restricted pregnant beef cows supports compensatory fetal muscle growth. J. Anim. Sci. 91, 4797–4806. https://doi.org/10.2527/jas.2013-6704.

Hales, C.N., Barker, D.J.P., 2001. The thrifty phenotype hypothesis. Br. Med. Bull. 60, 5–20. https://doi.org/10.1093/bmb/60.1.5.

He, Z.X., Wu, D.Q., Sun, Z.H., Tan, Z.L., Qiao, J.Y., Ran, T., Tang, S.X., Zhou, C.S., Han, X.F., Wang, M., Kang, J.H., Beauchemin, K.A., 2013. Protein or energy restriction during late gestation alters fetal growth and visceral organ mass: an evidence of intrauterine programming in goats. Anim. Reprod. Sci. 137, 177–182. https://doi.org/10.1016/j.anireprosci.2013.01.005.

Huang, D.W., Sherman, B.T., Lempicki, R.A., 2009. Bioinformatics enrichment tools: paths toward the comprehensive functional analysis of large gene lists. Nucleic Acids Res 37, 1–13. https://doi.org/10.1093/nas/gkn923.

Idrees, M., Xu, L., El Sheikh, M., Sidrat, T., Song, S.-.H., Joo, M.-.D., Lee, K.-.L., Kong, I.-.K., 2019. The PPARδ Agonist GW501516 Improves Lipolytic/Lipogenic Balance through CPT1 and PEPCK during the Development of Pre-Implantation Bovine Embryos. Int. J. Mol. Sci. 20, 6066. https://doi.org/10.3390/ijms20236066.

Imran, M., Lim, I.K., 2013. Regulation of Btg2/TIS21/PC3 expression via reactive oxygen species-protein kinase C-NFκB pathway under stress conditions. Cell. Signal. 25, 2400–2412. https://doi.org/10.1016/j.cellsig.2013.07.015.

Joo, S.T., Joo, S.H., Hwang, Y.H., 2017. The relationships between muscle fiber characteristics, intramuscular fat content, and fatty acid compositions in M. longissimus lumborum of Hanwoo steers. Korean J. Food Sci. Anim. Resour. 37, 780–786. https://doi.org/10.5851/kosfa.2017.37.5.780.

Kozakowska, M., Ciesla, M., Stefanska, A., Skrzypek, K., Was, H., Jazwa, A., Grochot-Przeczek, A., Kotlinowski, J., Szymula, A., Bartelik, A., Mazan, M., Yagensky, O., Florczyk, U., Lemke, K., Zebzda, A., Dyduch, G., Nowak, W., Szade, K., Stepniewski, J., Majka, M., Derlacz, R., Loboda, A., Dulak, J., Jozkowicz, A., 2012. Heme Oxygenase-1 inhibits myoblast differentiation by targeting myomirs. Antioxid. Redox Signal. 16, 113–127. https://doi.org/10.1089/ars.2011.3964.

Langmead, B., Salzberg, S.L., 2012. Fast gapped-read alignment with Bowtie 2. Nat. Methods 9, 357–359. https://doi.org/10.1038/nmeth.1923.

Lewin, A.M., Grieve, I.C., 2006. Grouping Gene Ontology terms to improve the assessment of gene set enrichment in microarray data. BMC Bioinformatics 7, 426. https://doi.org/10.1186/1471-2105-7-426.

Liu, J., Wu, X., Franklin, J.L., Messina, J.L., Hill, H.S., Moellering, D.R., Walton, R.G., Martin, M., Garvey, W.T., 2010. Mammalian Tribbles homolog 3 impairs insulin action in skeletal muscle: role in glucose-induced insulin resistance. Am. J. Physiol. - Endocrinol. Metab. 298, E565–E576. https://doi.org/10.1152/ajpendo.00467.2009.

Marcus, J., Popko, B., 2002. Galactolipids are molecular determinants of myelin development and axo–glial organization. Biochim. Biophys. Acta (BBA)-General Subj. 1573, 406–413. https://doi.org/10.1016/S0304-4165(02)00410-5.

McHugh, M.L., 2012. Interrater reliability: the kappa statistic. Biochem. medica Biochem. medica 22, 276–282.

Meng, S.J., Yu, L.J., 2010. Oxidative stress, molecular inflammation and sarcopenia. Int. J. Mol. Sci. 11, 1509–1526. https://doi.org/10.3390/ijms11041509.

Moisá, S.J., Shike, D.W., Shoup, L., Rodriguez-Zas, S.L., Loor, J.J., 2015. Maternal plane of nutrition during late gestation and weaning age alter Angus × Simmental offspring longissimus muscle transcriptome and intramuscular fat. PLoS ONE 10, e0131478. https://doi.org/10.1371/journal.pone.0131478.

NRC, 2007. Nutrient Requirements of Small Ruminants: sheep, Goats, Cervids, and New World Camelids. Natl. Res. Counc. 272–280. https://doi.org/10.17226/11654.

Obanda, D.N., Yu, Y., Wang, Z.Q., Cefalu, W.T., 2015. Modulation of sphingolipid metabolism with calorie restriction enhances insulin action in skeletal muscle. J. Nutr. Biochem. 26, 687–695. https://doi.org/10.1016/j.jnutbio.2015.01.007.

Paradis, F., Wood, K.M., Swanson, K.C., Miller, S.P., McBride, B.W., Fitzsimmons, C., 2017. Maternal nutrient restriction in mid-to-late gestation influences fetal mRNA expression in muscle tissues in beef cattle. BMC Genomics 18, 632. https://doi.org/10.1186/s12864-017-4051-5.

Pillon, N.J., Frendo-Cumbo, S., Jacobson, M.R., Liu, Z., Milligan, P.L., Bui, H.H., Zierath, J.R., Bilan, P.J., Brozinick, J.T., Klip, A., 2018. Sphingolipid changes do not underlie fatty acid-evoked GLUT4 insulin resistance nor inflammation signals in muscle cells. J. Lipid Res. 59, 1148–1163. https://doi.org/10.1194/jlr.M080788.

Prudente, S., Sesti, G., Pandolfi, A., Andreozzi, F., Consoli, A., Trischitta, V., 2012. The mammalian tribbles homolog TRIB3, glucose homeostasis, and cardiovascular diseases. Endocr. Rev. 33, 526–546. https://doi.org/10.1210/er.2011-1042.

Rouault, J.P., Falette, N., Guehenneux, F., Guillot, C., Rimokh, R., Wang, Q., Berthet, C., Moyret-Lalle, C., Savatier, P., Pain, B., Shaw, P., Berger, R., Samarut, J., Magaud, J. P., Ozturk, M., Samarut, C., Puisieux, A., 1996. Identification of BTG2, an antiproliferative p53-dependent component of the DNA damage cellular response pathway. Nat. Genet. 14, 482–486. https://doi.org/10.1038/ng1296-482.

Selak, M.A., Storey, B.T., Peterside, I., Simmons, R.A., 2003. Impaired oxidative phosphorylation in skeletal muscle of intrauterine growth-retarded rats. Am. J. Physiol. - Endocrinol. Metab. 285, E130–E137. https://doi.org/10.1152/ajpendo.00322.2002.

Sunadome, K., Yamamoto, T., Ebisuya, M., Kondoh, K., Sehara-Fujisawa, A., Nishida, E., 2011. Article ERK5 Regulates Muscle Cell Fusion through Klf Transcription Factors. Dev. Cell 20, 192–205. https://doi.org/10.1016/j.devcel.2010.12.005.

Team, R.C., 2013. R: A language and Environment For Statistical Computing.

Trapnell, C., Pachter, L., Salzberg, S.L., 2009. TopHat: discovering splice junctions with RNA-Seq. Bioinformatics 25, 1105–1111. https://doi.org/10.1093/bioinformatics/btp120.

Wang, C., Arrington, J., Ratliff, A.C., Chen, J., Horton, H.E., Nie, Y., Yue, F., Hrycyna, C. A., Tao, W.A., Kuang, S., 2019a. Mettl21c methylates and stabilizes Hspa8 1 Methyltransferase-like 21c methylates and stabilizes the heat shock protein HSPA8 in type I myofibers in mice. J. Biol. Chem. 294, 13718–13728. https://doi.org/10.1074/jbc.RA119.008430.

Wang, L.X., Zhu, X.M., Yao, Y.M., 2019b. Sestrin2: its Potential Role and Regulatory Mechanism in Host Immune Response in Diseases. Front. Immunol. 10, 2797. https://doi.org/10.3389/fimmu.2019.02797.

Wang, Y.X., Zhang, C.L., Yu, R.T., Cho, H.K., Nelson, M.C., Bayuga-Ocampo, C.R., Ham, J., Kang, H., Evans, R.M., 2004. Regulation of muscle fiber type and running endurance by PPARδ. PLoS Biol. 2 (10), e294. https://doi.org/10.1371/journal.pbio.0020294.

Wang, Z., Gerstein, M., Snyder, M., 2009. RNA-Seq: a revolutionary tool for transcriptomics. Nat. Rev. Genet. 10, 57–63. https://doi.org/10.1038/nrg2484.

Wiederstein, J.L., Nolte, H., Günther, S., Piller, T., Baraldo, M., Kostin, S., Bloch, W., Schindler, N., Sandri, M., Blaauw, B., Braun, T., Hölper, S., Krüger, M., 2018. Skeletal muscle-specific methyltransferase METTL21C trimethylates p97 and regulates autophagy-associated protein breakdown. Cell Rep. 23, 1342–1356. https://doi.org/10.1016/J.CELREP.2018.03.136.

Yang, H., Xu, X., Ma, H., Jiang, J., 2016. Integrative analysis of transcriptomics and proteomics of skeletal muscles of the Chinese indigenous Shaziling pig compared with the Yorkshire breed. BMC Genet. 17, 80. https://doi.org/10.1186/s12863-016-0389-y.

Yang, S., Wang, Y., Wang, L., Shi, Z., Ou, X., Wu, D., Zhang, X., Hu, H., Yuan, J., Wang, W., Cao, F., Liu, G., 2018. RNA-Seq reveals differentially expressed genes affecting polyunsaturated fatty acids percentage in the Huangshan Black chicken population. PLoS ONE 13, e0195132. https://doi.org/10.1371/journal.pone.0195132.

Yuniati, L., Scheijen, B., van der Meer, L.T., van Leeuwen, F.N., 2019. Tumor suppressors BTG1 and BTG2: beyond growth control. J. Cell. Physiol. 234, 5379–5389. https://doi.org/10.1002/jcp.27407.

Zhang, S., Regnault, T.R.H., Barker, P.L., Botting, K.J., McMillen, I.C., McMillan, C.M., Roberts, C.T., Morrison, J.L., 2015. Placental adaptations in growth restriction. Nutrients 7, 360–389. https://doi.org/10.3390/nu7010360.

Zhang, W., Garvey, J., Luo, N., Garvey, T., Fu, Y., 2014. MINOR (NR4A3) Overexpression in Mouse Skeletal Muscle Enhances Insulin Action. J. Mol. Genet. Med S. 1 https://doi.org/10.4172/1747-0862.s1-021, 1747-0862.

Zhou, L.Z.H., Johnson, A.P., Rando, T.A., 2001. NFκB and AP-1 mediate transcriptional responses to oxidative stress in skeletal muscle cells. Free Radic. Biol. Med. 31, 1405–1416. https://doi.org/10.1016/S0891-5849(01)00719-5.